

## QUANTITATIVE EVALUATION OF LATERAL FORCES ON THE PATELLA: STATIC AND KINEMATIC MAGNETIC RESONANCE IMAGING\*

Je Hoon Yang<sup>1</sup>, Guilherme Tadeu Sauaia Demarchi<sup>2</sup>, Emerson Garms<sup>3</sup>, Yara Juliano<sup>4</sup>, Luiz Aurélio Mestriner<sup>5</sup>, Moises Cohen<sup>6</sup>, Ricardo Dizioli Navarro<sup>6</sup>, Artur da Rocha Corrêa Fernandes<sup>7</sup>

**Abstract** **OBJECTIVE:** To evaluate the usefulness of combining static and kinematic magnetic resonance imaging in the evaluation of the femoropatellar joint. **MATERIALS AND METHODS:** Twenty healthy volunteers (40 knees) and 23 patients (43 knees) were submitted to both static and kinematic magnetic resonance imaging on a 1.5 tesla whole-body magnetic resonance scanner. The knees were positioned at 30° flexion with the quadrature knee coil at the inner end of the examination table. The patellar translation was evaluated by measurements of bisect offset, lateral patellar displacement and patellar tilt angle. The nonparametric Wilcoxon test was utilized for statistical analysis of data resulting from the static and kinematic studies in both groups. Nonparametric Mann-Whitney test was utilized in the comparison between healthy volunteers and patients. **RESULTS:** Statistical analysis demonstrated significant differences ( $p < 0.05$ ) between static and kinematic magnetic resonance imaging for the three parameters evaluated in both groups. Among the patients the differences between static and kinematic measurements were greater than those found in the volunteers, at 30° and 20° flexion, with bisect offset and lateral patellar displacement. **CONCLUSION:** Static and kinematic magnetic resonance imaging, when performed in association, demonstrated that the lateral forces being exerted on the patella are higher at a knee flexion at the range between 20° and 30°, particularly in individuals symptomatic for femoropatellar instability.

*Keywords:* Knee; Knee joint; Patella; Patellofemoral pain syndrome; Magnetic resonance imaging; Biomechanics; Chondromalacia patellae.

**Resumo** *Avaliação quantitativa das forças laterais da patela: ressonância magnética estática e cinemática.*

**OBJETIVO:** Avaliar a validade da ressonância magnética cinemática combinada com a ressonância magnética estática no estudo da articulação femoropatelar. **MATERIAIS E MÉTODOS:** Foram realizadas ressonância magnética estática e ressonância magnética cinemática em 20 voluntários assintomáticos (40 joelhos) e em 23 pacientes (43 joelhos), em aparelho de configuração fechada de 1,5 tesla de campo. Os indivíduos foram posicionados na extremidade da mesa, em 30° de flexão. A translação patelar foi avaliada medindo-se o desvio da bissetriz, o deslocamento lateral da patela e o ângulo de inclinação da patela. Para a comparação entre os estudos estático e cinemático, foi utilizado o teste não-paramétrico de Wilcoxon. Para a comparação entre os voluntários e os pacientes, foi utilizado o teste de Mann-Whitney. **RESULTADOS:** Houve diferenças significantes entre a ressonância magnética estática e a ressonância magnética cinemática ( $p < 0,05$ ) nos três parâmetros utilizados. No grupo dos pacientes, as diferenças entre a ressonância magnética estática e a ressonância magnética cinemática foram maiores que nos voluntários a 20° e a 30° de flexão, com o desvio da bissetriz e com o deslocamento lateral da patela. **CONCLUSÃO:** A combinação da ressonância magnética estática e ressonância magnética cinemática evidenciou que a força resultante lateral é maior na faixa de 20° e 30° de flexão, especialmente nos indivíduos sintomáticos, para a instabilidade femoropatelar.

*Unitermos:* Joelho; Articulação do joelho; Patela; Síndrome da dor patelofemoral; Imagem por ressonância magnética; Biomecânica; Condromalácia da patela.

\* Study developed in the Department of Imaging Diagnosis and Department of Orthopedics and Traumatology, Universidade Federal de São Paulo-Escola Paulista de Medicina (Unifesp-EPM), São Paulo, SP, Brazil.

1. Master in Clinical Radiology, MD, Collaborator, Department of Imaging Diagnosis, Universidade Federal de São Paulo-Escola Paulista de Medicina (Unifesp-EPM), São Paulo, SP, Brazil.

2. MD, Resident, Department of Imaging Diagnosis, Universidade Federal de São Paulo-Escola Paulista de Medicina (Unifesp-EPM), São Paulo, SP, Brazil.

3. Titular Member of Sociedade Brasileira de Ortopedia e Traumatologia, Assistant Physician, Department of Orthopedics and Traumatology, Universidade Federal de São Paulo-Escola Paulista de Medicina (Unifesp-EPM), São Paulo, SP, Brazil.

4. Associate Professor, Department of Preventive Medicine and

Biostatistics, Universidade Federal de São Paulo-Escola Paulista de Medicina (Unifesp-EPM), São Paulo, SP, Brazil.

5. Associate Professor, Department of Orthopedics and Traumatology, Universidade Federal de São Paulo-Escola Paulista de Medicina (Unifesp-EPM), São Paulo, SP, Brazil.

6. Private Docents, Professors, Department of Orthopedics and Traumatology, Universidade Federal de São Paulo-Escola Paulista de Medicina (Unifesp-EPM), São Paulo, SP, Brazil

7. Associate Professor, Department of Imaging Diagnosis, Universidade Federal de São Paulo-Escola Paulista de Medicina (Unifesp-EPM), São Paulo, SP, Brazil.

Mailing address: Dr. Je Hoon Yang, Rua Haddock Lobo, 144/42, São Paulo, SP, Brazil, 01414-000. E-mail: yang.rm@epm.br  
Received October 8, 2006. Accepted after revision January 15, 2007.

## INTRODUCTION

Anterior knee pain is a frequent complaint in the daily practice of orthopedists, especially from the young female population. Most frequently, femoropatellar instability is considered as the number-one cause of anterior knee pain<sup>(1-3)</sup>. Biomechanical evidence shows that the last 30° of extension are critical within the full

range in the femoropatellar joint dynamics. Lateral forces on the patella at this angle are higher, and so is the risk for subluxation<sup>(4)</sup>. Since 1941, when Wiberg developed the anatomical classification of the patella, several radiographic techniques for evaluating the femoropatellar joint at flexion angles 20° and 45° have been described<sup>(5-7)</sup>. The axial view of the patella at up to 30° flexion is difficult to perform, but many of the troublesome aspects only could be overcome by utilizing computed tomography (CT) and magnetic resonance imaging (MRI)<sup>(8,9)</sup>. Still, these techniques do not allow the evaluation of the femoropatellar joint with active quadriceps contraction and therefore many biomechanical aspects of the femoropatellar joint still remain to be appropriately studied. Kinematic MRI has recently emerged as a highly sensitive method to determine the presence of lateral displacement of the patella<sup>(10,11)</sup> ultimately supplying clinically significant information concerning femoropatellar joint dynamics.

To date, there is no report in the literature regarding the determination of the critical range of flexion concerning femoropatellar joint functional forces by means of cross-sectional tomographic images.

The present study was aimed at evaluating the validity of combining static and kinematic MRI in the dynamic study of the femoropatellar joint during active quadriceps contraction, correlating the resulting data with biomechanical fundamentals reported in the literature.

## MATERIALS AND METHODS

### Study population

Transversal study developed in the period between November/2001 and March/2003, evaluating 20 healthy volunteers (40 knees) and 25 patients (43 knees). The study was conducted in compliance with the Declaration of Helsinki VI (Edinburgh, October/2000) and under the approval of the Committee for Ethic in Research of Universidade Federal de São Paulo. Written free informed consent was obtained from all the participating individuals.

Asymptomatic volunteers: 10 men (20 knees), aged  $28.7 \pm 4.6$  years (mean  $\pm$  1 standard deviation [SD]); and 10 women (20 knees), aged  $28.4 \pm 4.7$  years (mean  $\pm$

1 SD) who had never visited a physician for knee-related complaints. Those who presented with a history of previous surgery or trauma involving the femoropatellar joint were excluded. Also, those with a ventral trochlear prominence on sagittal MRI reference images were excluded, considering that these factors constitute landmarks indicating higher risk for femoropatellar instability<sup>(12)</sup>.

The selection of patients was performed by specialized orthopedists among patients referred to our institution. Twenty-five consecutive patients (43 knees) presenting with femoropatellar instability were selected. The sample included eight knees in five male patients [age  $25 \pm 1.6$  years (mean  $\pm$  1 SD)] and 35 knees in 18 female patients [age  $21.6 \pm 6.4$  years (mean  $\pm$  1 SD)]. Physical examination demonstrated lateral hypermobility of the patella; increased lateralization of the patella during extension; positive apprehension test. All the female patients, one excepted, presented clinically with bilateral, not necessarily symmetrical, femoropatellar instability. Patients presenting with a history of acute traumatic dislocation or habitual dislocation of the patella, as well as those with a history of surgery in the knee, were excluded. Q-angle was not an inclusion criterion, considering the possibility of false-negative values in cases were not included in the selection criteria because such values could become falsely reduced in cases of patellar position-related abnormalities and valgism of extensor mechanisms<sup>(13)</sup>.

### Positioning

All of the volunteers and patients underwent both static and kinematic MRI in a 1.5 T whole-body MRI scanner (15 mT/m gradient strength) (Gyrosan ACS NT 15, Powertrak 1000; Philips Medical System, Best, Netherlands).

The knees were positioned at 30° flexion with the quadrature knee coil at the inner end of the examination table. Aiming at allowing this flexion arc, the knee was positioned at a height of 18 cm (coil base = 5 cm + foam cushion under the coil = 3 cm + examination table thickness = 10 cm). Lateral, but not rotatory, motion was restrained by the coil. Palpable external anatomical landmarks were adopted as refer-

ence points: the most prominent point of the greater trochanter; the lateral femorotibial joint space, a point located cranial and anteriorly to the fibular head; and the anterior margin of the tibial diaphysis. From these points two imaginary lines were determined: one between the greater trochanter and the lateral femorotibial joint space, and another parallel to the anterior margin of the tibial diaphysis. A universal 360° goniometer was positioned on the intersection between these two lines, and the intersection angle was considered as the knee flexion angle. Non-ferromagnetic, 1 cm-thick discs were placed under the ankle so that 30°, 20°, 10° flexion and full extension were achieved. After that, the examination table was inserted into the magnet bore (Figure 1).

### Images acquisition

Before static and kinematic MR images acquisition, effective knee flexion angles were measured on referential sagittal MR images, at the intersection between the greater axis of the femur and the anterior margin of the tibia. Images acquisition proceeded, provided the results of this measurement were between 26° and 34°.

Static MRI involved acquisition of sections at 30°, 20°, 10° flexion and at full extension. The number of discs under the ankles required to achieve these flexion degrees was determined as previously described. Axial, spin-echo T1-weighted sequences were performed with repetition time (RT)/echo time (ET) 457/13 ms; rectangular field-of-view (FOV), 90%; 256 × 160 image matrix on a 160 × 144 mm FOV; number of sections 19; section thickness/gap, 4.5/0.5 mm.

Kinematic MRI involved acquisitions at 1 cm, 2 cm, 3 cm, and 4 cm up from the lateral femorotibial joint space. The option for the lateral space took into consideration the lower curvature in relation to the medial femorotibial joint space (Figure 2)<sup>(14)</sup>. A turbo spin-echo sequence was performed with RT/ET 325/79 ms; rectangular FOV, 70%; 128 × 80 image matrix; 160 × 112 mm FOV; turbo factor, 24; section thickness, 8 mm. These parameters associated with a partial k-space reconstruction algorithm allowed an image to be obtained every 525 ms without motion artifacts. The

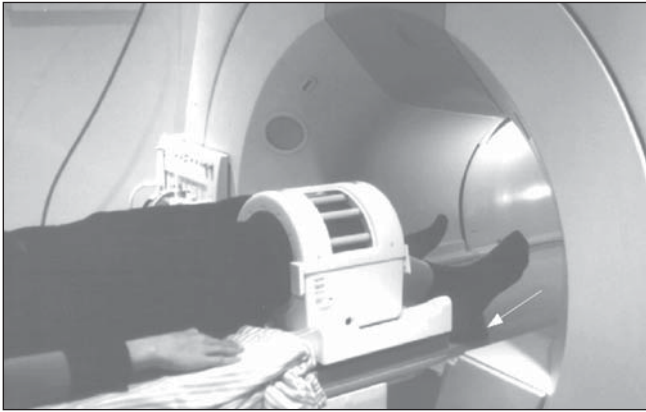


**Figure 1.** Female, 23-year old patient with 173 cm in height. Positioning a 30° knee flexion, with three non-ferromagnetic discs under the ankle (arrow).

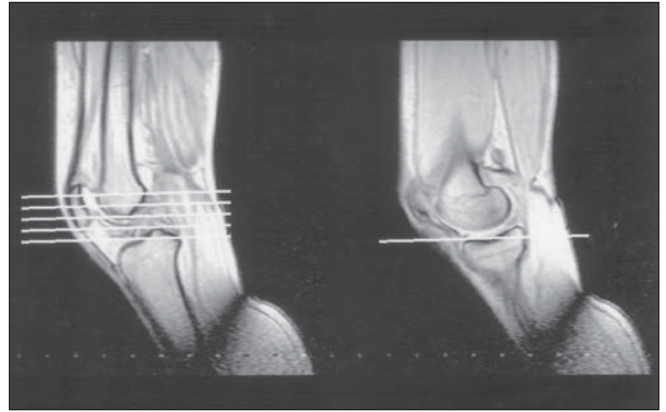


**Figure 2.** Kinematic RM images were acquired at 1 cm, 2 cm, 3 cm and 4 cm above the lateral femorotibial space.

individuals were given instructions to extend the knees from 30° flexion to full extension, starting and finishing according to the gradient switching noise. These movements were practiced before the effective images acquisition. The single-slice-multiphase technique generated eight sequential axial images in 4.2 seconds. Imaging was considered as satisfactory if uniform extension was achieved in all of the four planes. The entire process of a knee examination, including patients positioning, instructions, test runs, static and kinematic MRI, took about 25 minutes.

### Images evaluation

Each knee received an identification number and was separately evaluated.

Exact flexion angles could not be directly determined in the kinematic MRI, so “flexion sectors” instead of flexion degrees were adopted as reference. The 30° flexion range was divided into eight sectors (I to VIII), and each kinematic MRI frame was classified according to the estimated flexion range (Table 1).

The images corresponding to the same flexion sector in four kinematic MRI acquisitions were compared with the corresponding static MR images.

The transversal area of the *vastus medialis* muscle was adopted as a parameter indicating the presence of quadriceps contracture at kinematic MRI. Static RM images at 30° flexion were compared with those from the sector I of kinematic MRI, and the static MR images at full extension, with those from the sector VIII of kinematic

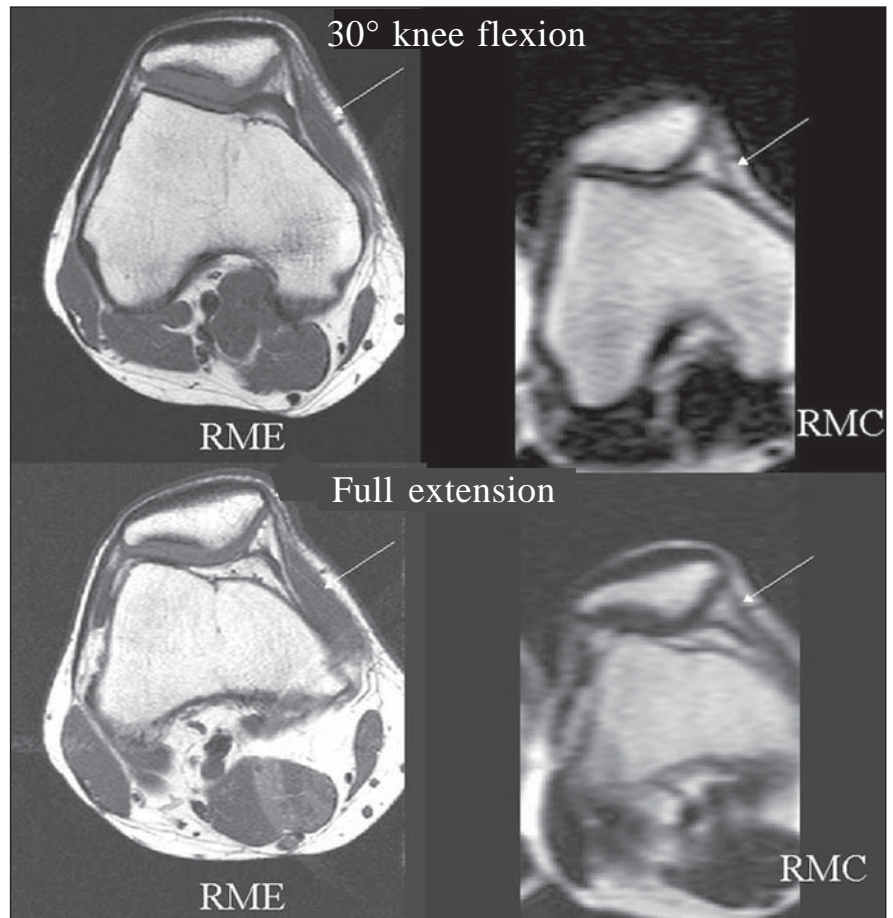


**Figure 3.** Static MRI (RME) and kinematic MRI (RMC) at 30° knee flexion and full extension. Transversal area of the vastus medialis muscle is smaller at kinematic MRI in both cases (arrows).

MRI. This comparison was made between images acquired from the corresponding distances from the lateral femorotibial joint space (Figure 3). A transversal area of the *vastus medialis* muscle at kinematic MRI smaller than that at static MRI constituted

an indication of the presence of quadriceps contraction.

### Quantitative analysis

Bisect offset (BSO), lateral patellar displacement (LPD) and patellar tilt angle



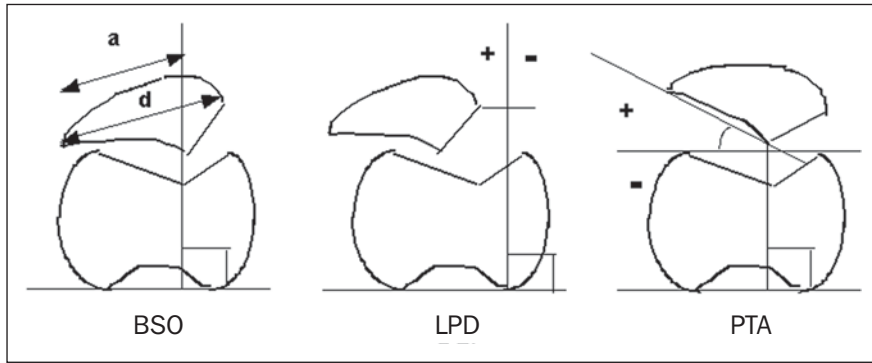


Figure 4. Quantitative analysis of the femoropatellar joint: BSO: a/d; LPD; PTA.

(PTA) were measured both on static and kinematic MRI<sup>(15)</sup> (Figure 4).

Two images from a same flexion degree (static MRI) or from a same flexion sector (kinematic MRI), acquired at 1 cm, 2 cm, 3 cm, and 4 cm up from the lateral femorotibial joint space, were selected for measurements: one demonstrating the largest transversal area of the patella, and the other, the most representative image of the intercondylar groove. Reference points were superposed utilizing the above mentioned parameters, according to Brossmann et al.<sup>(15)</sup>.

Data from asymptomatic volunteers and patients on both static and kinematic MRI were compared independently for each of the three parameters, and separately for each group of individuals (asymptomatic volunteers and patients) (Table 2). Considering that the static MRI presents four fixed flexion degrees, and the kinematic MRI, eight flexion sectors, the comparison was made as per Table 2.

A “delta” was defined, corresponding to the difference between parameters resulting from static and kinematic MRI. The values resulted from an arithmetical subtraction of variables for each parameter and for each individual (asymptomatic volunteers and patients). The results of this arithmetical subtraction for each parameter (BSO, LPD and PTA) were named BSO-delta, LPD-delta and PTA-delta for all the acquisitions at 30°, 20°, 10° and full extension of each knee. Flexion degrees and flexion sectors were combined (Table 2).

**Statistical analysis**

Considering the nature of the variables studied, non-parametric tests were utilized for statistical analysis.

Table 2 Measurements comparison: static MRI × kinematic MRI.

Static MRI measurements at	Kinematic MRI measurements
30°	Sector I (30°)
20°	Sectors III and IV mean values (<25° to ≥20° and <20° to ≥15°)
10°	Sectors V e VI mean values (<15° to ≥10° and <10° to ≥5°)
0°	Sector VIII (0°)

1. Asymptomatic volunteers *versus* patients – Non-parametric Mann-Whitney test for both static and kinematic MRI data.

2. Static *versus* kinematic MRI – Non-parametric Wilcoxon signed rank test for asymptomatic volunteers and patients, separately evaluated.

3. Asymptomatic volunteers *versus* patients for delta-parameters – Non-parametric Mann-Whitney test

Null hypothesis rejection level = 0.05 or 5% (statistical significance =  $p < 0.05$ ). Significant  $z$  and  $p$  values are marked with an asterisk.

**RESULTS**

**Asymptomatic volunteers *versus* patients**

Statistically significant differences ( $p < 0.05$ ) were found between measurements in asymptomatic volunteers and patients for the three parameters, both by static and kinematic MRI, at 30° flexion up to full extension.

**Static MRI *versus* kinematic MRI**

**Asymptomatic volunteers** – Differences found between static and kinematic MRI measurements were statistically significant for BSO and LPD at 20° and 10° flexion. For PTA, statistically significant

Table 1 Image and corresponding flexion sector, and estimated flexion angle at kinematic MRI.

Kinematic image	Flexion sector	Estimated flexion angle
First image	I	30°
Second image	II	<30° to ≥25°
Third image	III	<25° to ≥20°
Fourth image	IV	<20° to ≥15°
Fifth image	V	<15° to ≥10°
Sixth image	VI	<10° to ≥5°
Seventh image	VII	<5° to >0°
Eighth image	VIII	0°

differences were found at 30° and 20° flexion ( $p < 0.05$ ).

**Patients** – Differences found between static and kinematic MRI measurements were statistically significant for BSO and LPD from 30° flexion up to full extension. For PTA, statistically significant differences were not found. Patients showed significantly higher mean values for LPT by static MRI than asymptomatic volunteers. Kinematic MRI did not present significant variations (Table 3).

**Delta-parameters, asymptomatic volunteers *versus* patients**

Statistically significant differences were found between findings in asymptomatic volunteers and patients for BSO-delta and LPD-delta at 30° and 20° flexion ( $p < 0.05$ ). No statistically significant difference was found for PTA-delta (Table 4).

**DISCUSSION**

The results of the present study demonstrate statistically significant differences at 30° and 20° flexion for BSO-delta and LPD-delta, thus indicating that the lateral and medial forces on the patella were higher in the patients group at these flexion degrees. These parameters result from the arithmetical subtraction of values re-

**Table 3** Measurements comparison: static MRI × kinematic MRI — BSO, LPD and PTA for asymptomatic volunteers and patients.

	Degrees flexion sectors	Asymptomatic volunteers		Patients	
		z*	p*	z*	p*
BSO	30°	-1.116	0.264	-3.065†	0.002†
	20°	-2.308†	0.021†	-4.545†	0.000†
	10°	-4.650†	0.000†	-4.830†	0.000†
	0°	-3.324†	0.001†	-3.631†	0.000†
LPD	30°	-0.844	0.399	-3.185†	0.001†
	20°	-2.687†	0.007†	-3.441†	0.001†
	10°	-5.054†	0.000†	-3.860†	0.000†
	0°	-3.031†	0.002†	-3.691†	0.000†
PTA	30°	-3.035†	0.002†	-1.057	0.291
	20°	-2.537†	0.010†	-1.459	0.145
	10°	-1.796	0.073	-1.019	0.308
	0°	-0.763	0.466	-1.031	0.303

\* Calculated with the Wilcoxon signed rank test. † Statistically significant difference (p < 0.05). BSO, bisect offset; LPD, lateral patellar displacement; PTA, patellar tilt angle.

**Table 4** Comparison of BSO-delta, LPD-delta and PTA-delta between asymptomatic volunteers and patients.

	Angle flexion sector	Mean (standard deviation)		z*	p*
		Asymptomatic volunteers	Patients		
Delta-BSO	30°	0.06 (0.04)	0.10 (0.08)	-2.361†	0.018†
	20°	0.06 (0.06)	0.12 (0.09)	-3.206†	0.001†
	10°	0.09 (0.07)	0.13 (0.10)	-1.729	0.084
	0°	0.08 (0.06)	0.10 (0.11)	-0.196	0.084
Delta-LPD	30°	0.41 (3.18)	2.17 (6.34)	-2.520†	0.012†
	20°	1.25 (3.08)	3.40 (5.87)	-2.457†	0.014†
	10°	3.15 (3.63)	3.55 (6.25)	-0.571	0.568
	0°	2.33 (4.21)	3.46 (5.23)	-1.356	0.175
Delta-PTA	30°	4.99 (4.27)	6.37 (5.50)	-0.842	0.400
	20°	4.81 (4.25)	7.24 (7.09)	-1.081	0.279
	10°	5.38 (3.46)	5.69 (4.81)	-0.324	0.748
	0°	5.48 (5.12)	5.77 (5.34)	-0.347	0.728

\* Calculated with the Wilcoxon signed rank test. † Statistically significant difference (p < 0.05). BSO, bisect offset; LPD, lateral patellar displacement; PTA, patellar tilt angle.

sulting from measurements by static and kinematic MRI, with and without active quadriceps muscle contraction.

These data are compatible with those reported in a study about the femoropatellar dynamics. In the last 30° of extension, the tibial tubercle rotates externally, generating tension over the quadriceps tendon and the patella is laterally dislocated, thus increasing the femoropatellar contact pressure<sup>(16-18)</sup>. Tension on the lateral retinaculum is maximal between 30° and 20° flexion, and so is the risk of subluxation<sup>(1,11,19)</sup>.

Static sectional images, with “loaded quadriceps” could do the same, but this is

not a consensus. Sasaki & Yagi and Schutzer et al. demonstrated greater LPD and PTA under quadriceps contraction at static CT<sup>(20,21)</sup>, but the classification of Schutzer et al. for patients affected by femoropatellar pain has not considered quadriceps contraction<sup>(22)</sup>. Delgado-Martínez et al. have reported that CT scans performed with under quadriceps contraction did not provide any significant information as compared with “unloaded quadriceps” imaging modalities<sup>(23)</sup>.

There are several quantitative parameters described for evaluation of femoropatellar joint, but with no consensus in the

literature. Finding reliable anatomical references, as well as performing appropriate measurements, not always is feasible<sup>(24)</sup>. A subjective evaluation could be an alternative. Apparently, it would be easier to distinguish between different grades of lateral subluxation, with low inter-observer variation<sup>(11)</sup>, however, such approach could not be adopted in the present study due to the absence of accurate references to allow data reproducibility in the comparison between static and kinematic MRI.

The posterior intercondylar plane was adopted for all of the three parameters. It has the advantage of not being affected by the presence of hypoplastic lateral femoral condyles<sup>(23)</sup>. On the other hand, according Delgado-Martínez et al., the inter- and intra-observer correlation coefficients were higher when the anterior intercondylar plane was adopted<sup>(24)</sup>.

A reliable method for measuring patellar tracking is still to be achieved, and, also, a definition for patellar normality is still to be found<sup>(25,26)</sup>. Reference values reported for static MRI are not valid for kinematic MRI, considering that mild lateral subluxation undetectable by static MRI can be found at kinematic MRI at full extension<sup>(27)</sup>. Brossmann et al. have reported statistically significant differences between static and kinematic MRI in the group of asymptomatic volunteers for BSO and PTA from 10° flexion up to full extension<sup>(15)</sup>. The findings of the present study are very similar. Statistically significant differences were found for all of the three parameters in this flexion range. For BSO and PLD these findings were observed from 20° flexion up to full extension. According to Kujala et al., female and male femoropatellar joint behave differently at static MRI<sup>(9)</sup>. According to Csintalan et al. there are significant differences between female and male femoropatellar joint biomechanics<sup>(28)</sup>. These aspects emphasize the necessity of further studies to define reference values for both healthy female and male groups.

An aspect to be emphasized in the present study is the coil positioning. According to McNally and Muhle et al., current MRI devices, in closed configuration, allow movement amplitude between 30° flexion up to full extension<sup>(11,29)</sup>. In the present study, there was a concern whether

there was enough space for all of the individuals if they were positioned as above mentioned. The system suggested by the present study certainly the available space is larger because the coil is placed 3 cm above the inner end of the examination table, so the knee movement can be easily achieved in a greater space inside the magnet bore that otherwise would be occupied by the examination table.

Images acquisition was performed in dorsal decubitus with no resistance to extension. In ventral decubitus, the patella would be fixed on the examination table, and its movement would therefore be constrained<sup>(11)</sup>. Individuals positioning and images acquisition were performed with no specific positioning device. However, in strict compliance with previously defined standards for both anatomical landmarks and examination methods, images acquisition was allowed within these same standards so reducing the probability of sequential errors. In the absence of a specially designed positioning device, a two-step evaluation was required. The first step was aimed at ensuring *quasi* 30° of knee flexion, and the second one, ensuring active quadriceps contraction along the whole extension movement during the kinematic MRI examination. A significant part of the time was spent on this alone. It has even been considered constructing a special positioning device, however, at such an early stage of the project, the decision was to apply the aforementioned system first and check its feasibility, postponing the construction of a specific device to the future.

McNally<sup>(11)</sup> and Shellock et al.<sup>(30)</sup> utilized a quadrature body coil, and Brossmann et al., a surface RF coil<sup>(10,15)</sup>. Surface coils achieve a higher signal/noise ratio over a limited field of view. On the other hand, the homogeneous signal reception presented by the quadrature coil, is absent in surface coils<sup>(31)</sup>. A dedicated quadrature knee coil seems to be the natural option, considering the better signal/noise ratio in relation to the body coil, with a more homogeneous signal as compared with the surface coil. A dedicated quadrature knee coil, however, is not devoid of drawbacks — aiming at enabling free extension of the knee the patella was placed near its inner

end of the coil (Figure 1C) so the final position of the outer coil end is on the middle portion of the thigh. Its diameter restriction may not allow the examination of all patients. At least in the present study, the majority of patients with clinical femoropatellar syndrome were young women with relatively thin thighs and therefore all the examinations could be performed without any hindrance.

Considering a single radiologist who was aware of the clinical data performed all the measurements, the interobserver variability could not be evaluated. With a small study group like the present one, sampling homogeneity becomes a critical issue. All of the patients demonstrated clear clinical signs of femoropatellar instability, the majority of them bilateral. As a result, an independent statistical analysis for both male and female individuals could not be performed.

It should be emphasized that several phases of data handling are required before delta-parameters are defined. Concern is raised about systematic errors that could possibly be generated throughout the process. Nonparametric tests have less test power for null hypothesis rejection, and also are often more conservative than the parametric tests<sup>(32)</sup>.

This new positioning system, along with the static MRI/kinematic MRI combination could become a very sensitive method for the evaluation of biomechanical femoropatellar disorders.

## CONCLUSION

Kinematic MRI, when performed in association with static MRI, demonstrates that there are greater lateral forces being exerted on the patella at a 30° to 20° range of knee flexion, particularly in individuals symptomatic for femoropatellar instability. These evidences demonstrate the potential clinical usefulness of adding kinematic MRI to the arsenal for evaluating the femoropatellar joint in patients suspicious for femoropatellar instability with no significant finding at static MRI.

## Acknowledgments

The authors would like to acknowledge the support of the Coordenadoria de

Aperfeiçoamento do Pessoal de Nível Superior (Capes) – Conselho Nacional de Educação (National Education Council), Ministry of Education, Brazil.

## REFERENCES

- Inoue M, Shino K, Hirose H, Horibe S, Ono K. Subluxation of the patella. Computed tomography analysis of patellofemoral congruence. *J Bone Joint Surg Am* 1988;70:1331–1337.
- Lin F, Wang G, Koh JL, Hendrix RW, Zhang LQ. In vivo and noninvasive three-dimensional patellar tracking induced by individual heads of quadriceps. *Med Sci Sports Exerc* 2004;36:93–101.
- Wilk KE, Briem K, Reinold MM, Devine KM, Dugas J, Andrews JR. Rehabilitation of articular lesions in the athlete's knee. *J Orthop Sports Phys Ther* 2006;36:815–827.
- Hungerford DS, Barry M. Biomechanics of the patellofemoral joint. *Clin Orthop Relat Res* 1979;(144):9–15.
- Wiberg G. Roentgenographic and anatomic studies on the femoropatellar joint. With special reference to chondromalacia patellae. *Acta Orthop Scand* 1941;12:319–410.
- Merchant AC, Mercer RL, Jacobsen RH, Cool CR. Roentgenographic analysis of patellofemoral congruence. *J Bone Joint Surg Am* 1974;56:1391–1396.
- Maldague B, Malghem J. Radiologie de l'instabilité rotulienne: intérêt du cliché de profil et de la vue axiale à 30° rotation externe. *Acta Orthop Belg* 1989;55:311–329.
- Delgado-Martins H. A study of the position of the patella using computerised tomography. *J Bone Joint Surg Br* 1979;61-B:443–444.
- Kujala UM, Österman K, Korman M, Komu M, Schlenzka D. Patellar motion analyzed by magnetic resonance imaging. *Acta Orthop Scand* 1989;60:13–16.
- Brossmann J, Muhle C, Büll CC, et al. Cine MR imaging before and after realignment surgery for patellar maltracking – comparison with axial radiographs. *Skeletal Radiol* 1995;24:191–196.
- McNally EG. Imaging assessment of anterior knee pain and patellar maltracking. *Skeletal Radiol* 2001;30:484–495.
- Pfirmann CWA, Zanetti M, Romero J, Hodler J. Femoral trochlear dysplasia: MR findings. *Radiology* 2000;216:858–864.
- Fithian DC, Mishra DK, Balen PF, Stone ML, Daniel DM. Instrumented measurement of patellar mobility. *Am J Sports Med* 1995;23:607–615.
- Warwick R, William P. *Gray's Anatomy*. 35th ed. Edinburgh: Longman Group Limited, 1973;391–394, 450–460.
- Brossmann J, Muhle C, Schröder C, et al. Patellar tracking patterns during active and passive knee extension: evaluation with motion-triggered cine MR imaging. *Radiology* 1993;187:205–212.
- Reilly DT, Martens M. Experimental analysis of the quadriceps muscle force and patello-femoral joint reaction force for various activities. *Acta Orthop Scand* 1972;43:126–137.
- Kumagai M, Mizuno Y, Mattessich SM, Elias JJ, Cosgarea AJ, Chao EY. Posterior cruciate ligament rupture alters in vitro knee kinematics. *Clin Orthop Relat Res* 2002;(395):241–248.
- Li G, DeFrate LE, Zayontz S, Park SE, Gill TJ. The effect of tibiofemoral joint kinematics on

- patellofemoral contact pressures under simulated muscle loads. *J Orthop Res* 2004;22:801–806.
19. Grood ES, Suntay WJ, Noyes FR, Butler DL. Biomechanics of the knee-extension exercise. Effect of cutting the anterior cruciate ligament. *J Bone Joint Surg Am* 1984;66:725–734.
  20. Sasaki T, Yagi T. Subluxation of the patella. Investigation by computerized tomography. *Int Orthop* 1986;10:115–120.
  21. Schutzer SF, Ramsby GR, Fulkerson JP. The evaluation of patellofemoral pain using computerized tomography. A preliminary study. *Clin Orthop Relat Res* 1986;(204):286–293.
  22. Schutzer SF, Ramsby GR, Fulkerson JP. Computed tomographic classification of patellofemoral pain patients. *Orthop Clin North Am* 1986;17:235–248.
  23. Delgado-Martínez AD, Estrada C, Rodríguez-Merchán EC, Atienza M, Ordóñez JM. CT scanning of the patellofemoral joint. The quadriceps relaxed or contracted? *Intern Orthop* 1996;20:159–162.
  24. Delgado-Martínez AD, Rodríguez-Merchán EC, Ballesteros R, Luna JD. Reproducibility of patellofemoral CT scan measurements. *Intern Orthop* 2000;24:5–8.
  25. Katchburian MV, Bull AMJ, Shih YF, Heatley FW, Amis AA. Measurement of patellar tracking: assessment and analysis of the literature. *Clin Orthop Relat Res* 2003;(412):241–259.
  26. Laprade J, Lee R. Real-time measurement of patellofemoral kinematics in asymptomatic subjects. *Knee* 2005;12:63–72.
  27. O'Donnell P, Johnstone C, Watson M, McNally E, Ostlere S. Evaluation of patellar tracking in symptomatic and asymptomatic individuals by magnetic resonance imaging. *Skeletal Radiol* 2005;34:130–135.
  28. Csintalan RP, Schulz MM, Woo J, McMahon PJ, Lee TQ. Gender differences in patellofemoral joint biomechanics. *Clin Orthop Relat Res* 2002;(402):260–269.
  29. Muhle C, Brossmann J, Heller M. Kinematic CT and MR imaging of the patellofemoral joint. *Eur Radiol* 1999;9:508–518.
  30. Shellock FG, Foo TKF, Deutsch AL, Mink JH. Patellofemoral joint: evaluation during active flexion with ultrafast spoiled GRASS MR imaging. *Radiology* 1991;180:581–585.
  31. Welker KM, Tsuruda JS, Hadley JR, Hayes CE. Radio-frequency coil selection for MR imaging of the brain and skull base. *Radiology* 2001;221:11–25.
  32. Applegate KE, Tello R, Ying J. Hypothesis testing III: counts and medians. *Radiology* 2003;228:603–608.